Angewandte Chemie
Eine Zeitschrift der Gesellschaft Deutscher Chemiker

Supporting Information

The Common Intermediates of Oxygen Evolution and Dissolution Reactions during Water Electrolysis on Iridium

Olga Kasian, Jan-Philipp Grote, Simon Geiger, Serhiy Cherevko, and Karl J. J. Mayrhofer*

anie_201709652_sm_miscellaneous_information.pdf

Experimental Procedures

Thin films of Ir were deposited by magnetron sputtering in Ar atmosphere (BESTEC GmbH, Berlin, Germany) at room temperature and 100 W. To prepare films with a minimal surface roughness, on the smooth substrates of single crystalline Si(100) wafers with a 1.5 μm thermal SiO_2 diffusion and reaction barrier layer were used. The base vacuum before deposition was $2.5x10^{-6}$ Pa. During the sputtering the pressure was adjusted to 0.5 Pa. The Ø3 inch target of Ir (99.9%, Evochem, Germany) was pre-cleaned by sputtering prior to deposition. The resulting thickness of the obtained coating was approximately 100 nm. Reactively sputtered oxide was deposited at 100 W in a mixture of O_2 and Ar as the sputter gas and the chamber pressure was regulated to 0.5 Pa at room temperature. Thermal oxide was prepared by thermal treatment of sputtered film of metallic Ir in air at 600^0C during 5 hours. The composition of the film was confirmed using X-ray diffraction (XRD) and X-ray photoelectron spectroscopy (XPS).

XPS measurements were performed (Quantera II, Physical Electronics, Chanhassen, MN, USA) applying a monochromatic Al Kα X-ray source (1486.6 eV) and operating at 15 kV and 25 W. The binding energy scale was referenced to the C 1s signal at 285.0 eV. Casa XPS software was used to analyze the experimentally obtained spectra. The fitting of spectra was performed after subtraction of a Shirley background. In all fits, the peak separation and the peak area ratios between the Ir 4f7/2 and the Ir 4f5/2 components were constrained to 3 eV and 4:3, respectively. A Doniach-Šunjic profile with an asymmetry parameter of 0.1 and a spectrum convolution width of 230 was used for the peak fittings. Detailed discussion of Ir XP spectra interpretation can be found in the literature.[1]

The prepared Ir metallic and oxide films served as the working electrodes in the scanning flow cell – inductively coupled plasma mass spectrometer (ICP-MS, NexION 300X, Perkin Elmer) based setup (Figure S1a), as described in.[2] All presented data are normalized to the geometric area of the working electrode (4.5×10^{-2} cm^2) assuming low roughness of the sputtered films. A graphite rod, placed in the inlet channel of the SFC, was utilized as the counter electrode. A saturated Ag/AgCl electrode (Metrohm, Germany) was used as the reference electrode. All reported potentials are referenced to the reversible hydrogen electrode (RHE) potential, which was measured in each day of experiments using a polycrystalline platinum foil (99.99%, MaTeck, Germany) in hydrogen saturated 0.1 M $HClO_4$. This solution was prepared by dilution of concentrated acid (Suprapur® 70% $HClO_4$, Merck, Germany) in ultrapure water (PureLab Plus system, Elga, 18 MΩcm, TOC < 3 ppb) and, after saturation with Ar, was also used in all electrochemical measurements. Prior to introduction into the ICP-MS the electrolyte was mixed with an internal standard of 10 μg L^{-1} of ^{187}Re in a Y-connector (mixing ratio 1:1) after the electrochemical cell. The ICP-MS was calibrated every day of experiment prior to the electrochemical measurements.

The volatile products were measured using scanning flow cell – on-line electrochemical mass spectrometer set up, previously described in.[3] In comparison to SFC connected to the ICP-MS, here the PTFE tip from the top of the cell through an extra vertical channel was introduced (Figure S1b). In this case, surface area of the working electrode was 12.5×10^{-2} cm^2. A 50 μm thick PTFE Gore-Tex membrane with a pore size of 20 nm, through which products can evaporate into the vacuum system of the mass spectrometer, was mounted onto the very end of the tip. The approximate distance from the tip to the electrode was about 50 μm, which is determined by the thickness of the silicon ring sealing around the cell opening and the applied contact force. These parameters affect the sensitivity and, therefore, they were kept constant during the whole set of measurements. The small size of pores and the thickness of the membrane result in the reduction of the water background pressure inside the vacuum and provide a good response time. Such optimized configuration results in good response time and high sensitivity. Considering that measured volatile species are unstable and are not available commercially, the calibration of mass spectrometer to recalculate measured intensities of formed IrO_3 into concentrations cannot be performed. Presented data, therefore, has rather qualitative than quantitative meaning. The SFC connected to analytics set-ups has a limitation in conditions when the formation of oxygen bubbles is intense. The gas bubbles may block working electrode, leading to potentiostat overloads. In case of OLEMS the oxygen bubbles may lead to artificial increase in the measured signal. The measurement of any signal with high mass to charge ratio can confirm the absence of the artificial increase in the measured intensity (e.g. m/z 246 in Figure S5). Considering essential difference in activities of studied Ir electrodes, the measurements were performed in galvanostatic conditions when formation of oxygen bubbles is comparable regardless the anode material.

A potentiostat (Gamry Reference 600, USA) was used for the electrochemical measurements with both setups. Each measurement was reproduced at least three times.

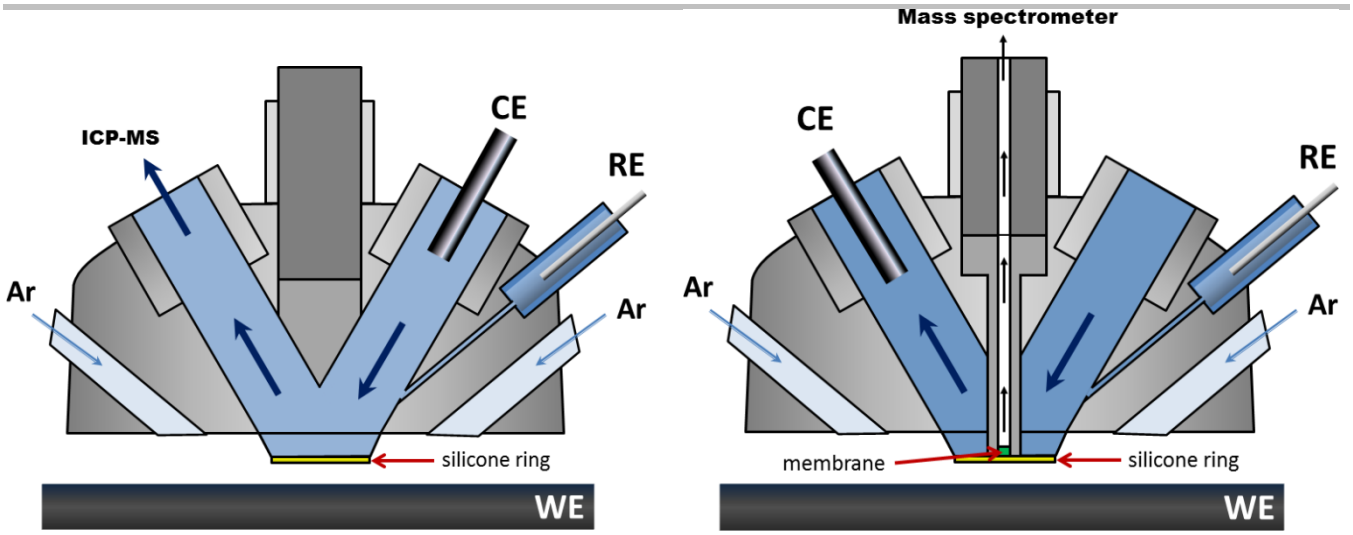

Figure S1. Schematic representation of SFC-ICP-MS and SFC-OLEMS setups.

Results and Discussion

To ensure composition of prepared electrodes XPS measurements were performed. Figure S2 shows XP spectra of Ir 4f and O 1s levels of as prepared metallic Ir film. In Figure S2a peak position at 60.9 eV corresponds to Ir^0.[1b,4] Considering, that electrode was exposed to air prior to XPS measurements O 1s spectrum shows OH groups and water molecules at the surface of electrode.

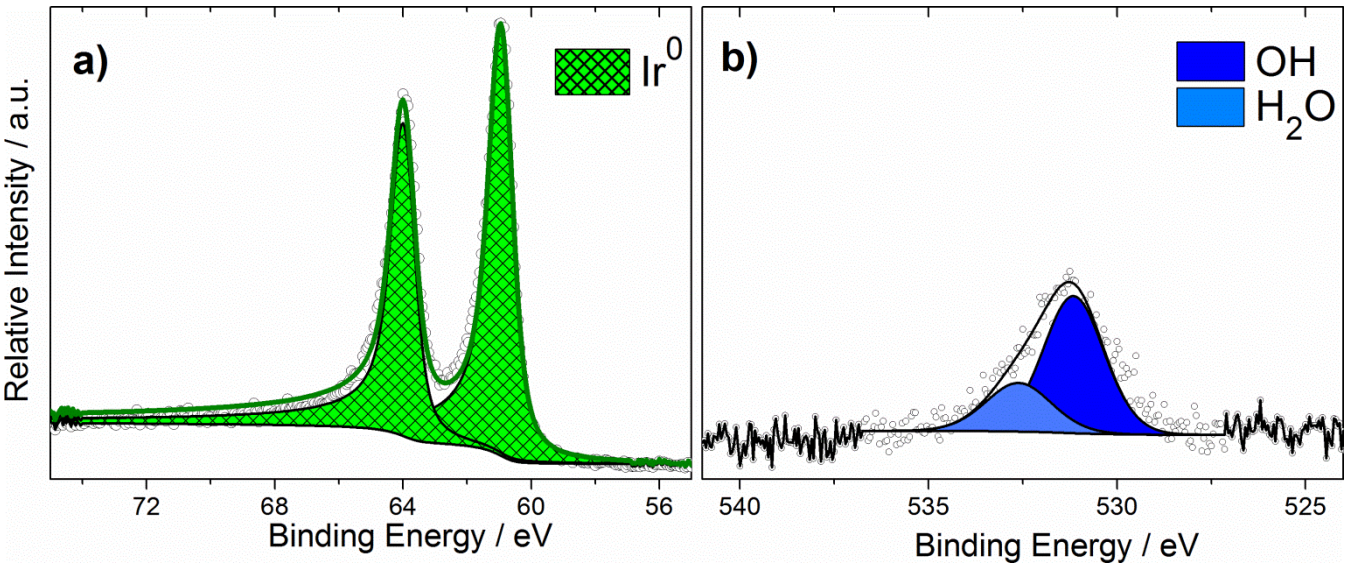

Figure S2. XP spectra of a) Ir 4f and b) O 1s levels for metallic Ir electrode.

XPS data of reactively sputtered Ir oxide are presented in Figure S3. The Ir $4f_{7/2}$ binding energy is 61.8 eV corresponding to IrO_2.[1c,4a] Detailed deconvolution of the Ir 4f spectra shows that Ir^{IV} is the only oxidation state of element in this sample. Spectra of O 1s level shows significant contribution of lattice oxygen (529.9 eV) in reactively sputtered oxide. Depth profiling with Ar does not show any change in XP spectra, ensuring similarity of surface and bulk composition.

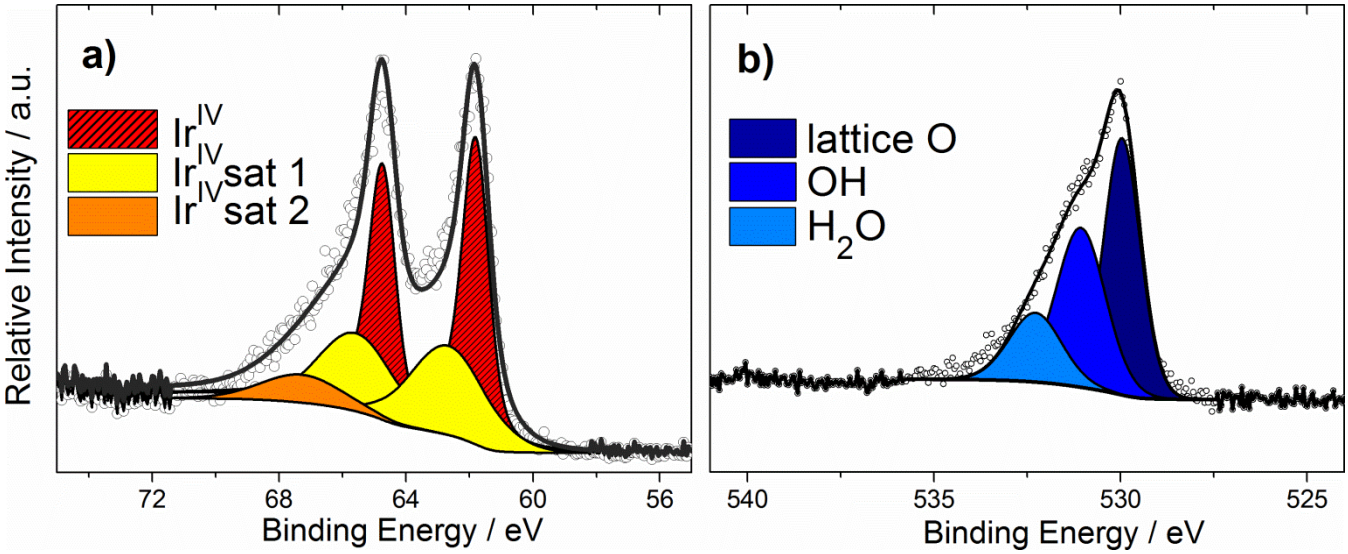

Figure S3. XP spectra of a) Ir 4f and b) O 1s levels for reactively sputtered oxide.

XP spectra of thermally prepared oxide (Figure S4) show the same peak positions and peak ratios as was observed for reactively sputtered oxide, indicating that thermal treatment of Ir in air leads to formation of IrO_2 on the electrode surface. As was shown in our previous work, the thickness of oxide film prepared in such conditions is about 10 nm,[5] which can be considered as a bulk oxide in electrochemical measurements.

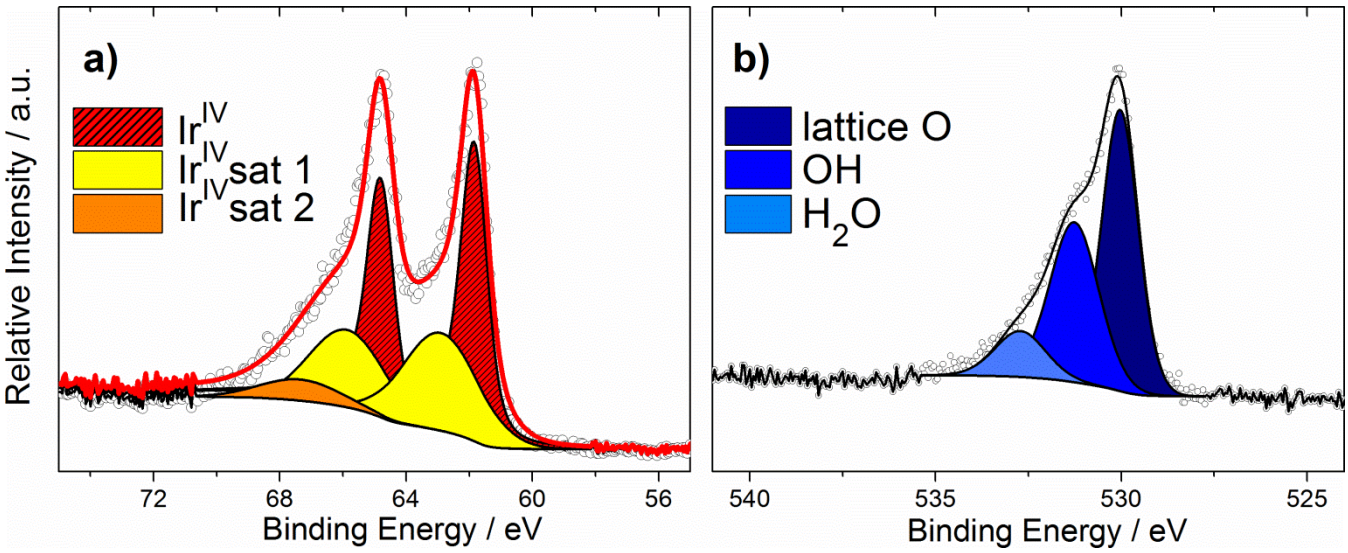

Figure S4. XP spectra of a) Ir 4f and b) O 1s levels for Ir thermal oxide.

Figure S5 shows data obtained during 30 s of polarization of thermally formed Ir oxide at 10, 15 and 20 mA cm^{-2}. The volatile species with mass to charge ratios (m/z) of 32 (c) and 240 (d) formed during the OER were measured in-situ using the SFC-OLEMS setup and correspond to O_2 and IrO_3, respectively. Signal with mass to charge ratio (m/z) of 246 was recorded to confirm the absence of artificial increase in the measured signals.

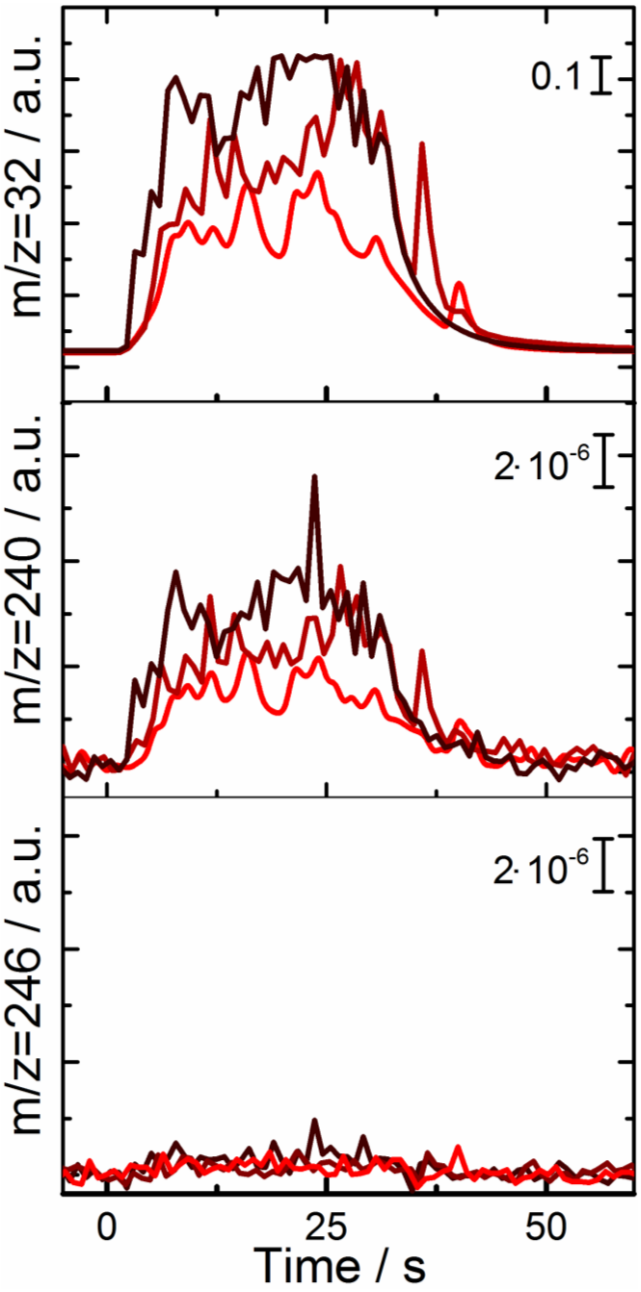

Figure S5. OLEMS measurements performed during the OER on Ir thermal oxide in 0.1 M $HClO_4$ at 10, 15 and 20 mA cm^{-2} and room temperature. Colour gradient indicates increase of measured current density from 10 to 20 mA cm^{-2}.

Figure S6 shows data obtained during 30 s of polarization of metallic Ir at 5, 10, 15 or 20 mA cm^{-2}. Corresponding values of potential (a), amount of dissolved Ir (b) were measured on-line using SFC-ICP-MS. The volatile species with mass to charge ratios (m/z) of 32 (c) and 240 (d) formed during the OER were measured in-situ during the same electrochemical protocol using the SFC-OLEMS setup and correspond to O_2 and IrO_3, respectively. Here, formation of IrO_3 is almost absent at current densities below 15 mA cm^{-2} and starts increasing at higher currents owing to dramatic increase in potential. Analogues data obtained for reactively sputtered IrO_2 is shown in Figure S7. Dissolution of reactively sputtered IrO_2 is slightly increasing with increasing current density, while formation of IrO_3 does not increase much, probably owing to low value of electrode potential (Figure S7a,d).

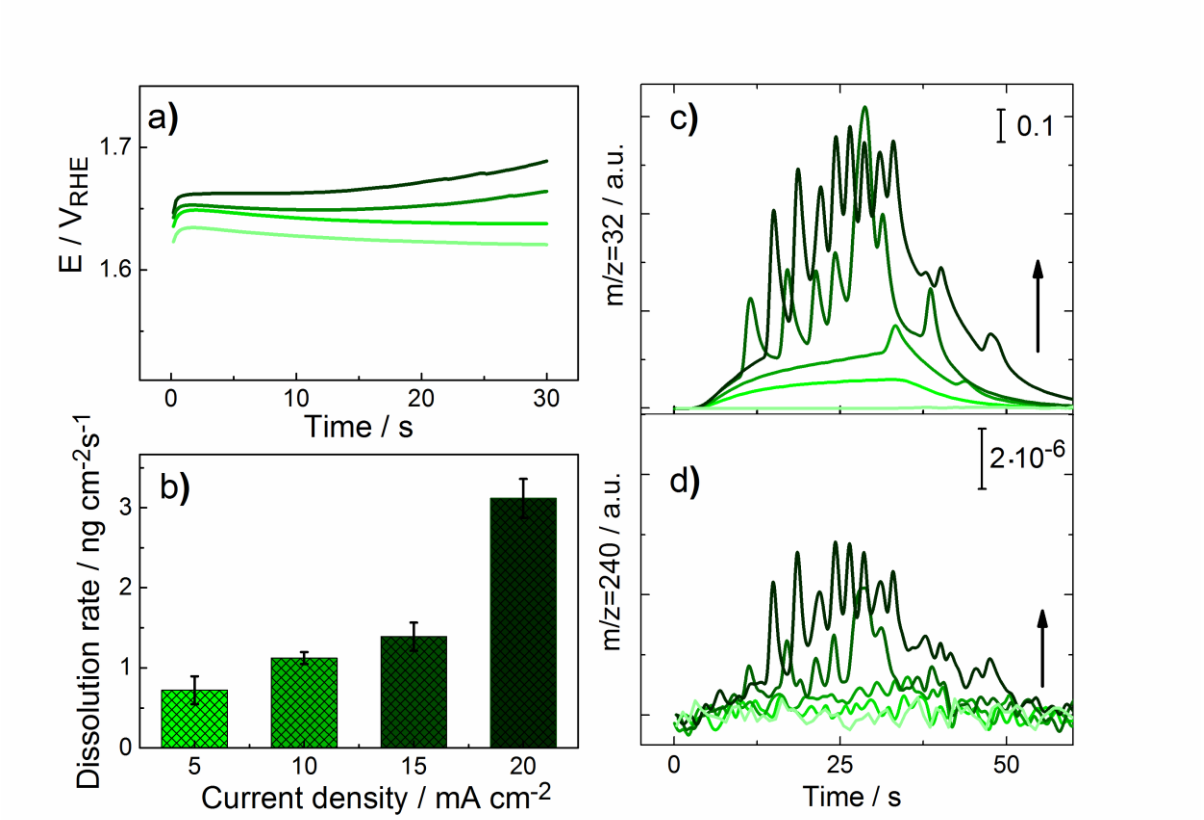

Figure S6. Direct observation of an intermediate of Ir dissolution during the OER. a) Measured potential during 30 s of anodic polarization of metallic Ir in 0.1 M $HClO_4$ at 5, 10, 15 and 20 mA cm^{-2} at room temperature. b) Rate of iridium dissolution and signals of c) $^{32}O_2$ and d) $^{240}IrO_3$ measured online with a). Gradient of colour indicates increase of applied current density from 5 mA cm^{-2} till 20 mA cm^{-2}. The baselines in c) and d) show the $^{32}O_2$ and $^{240}IrO_3$ signals measured at the open circuit potential.

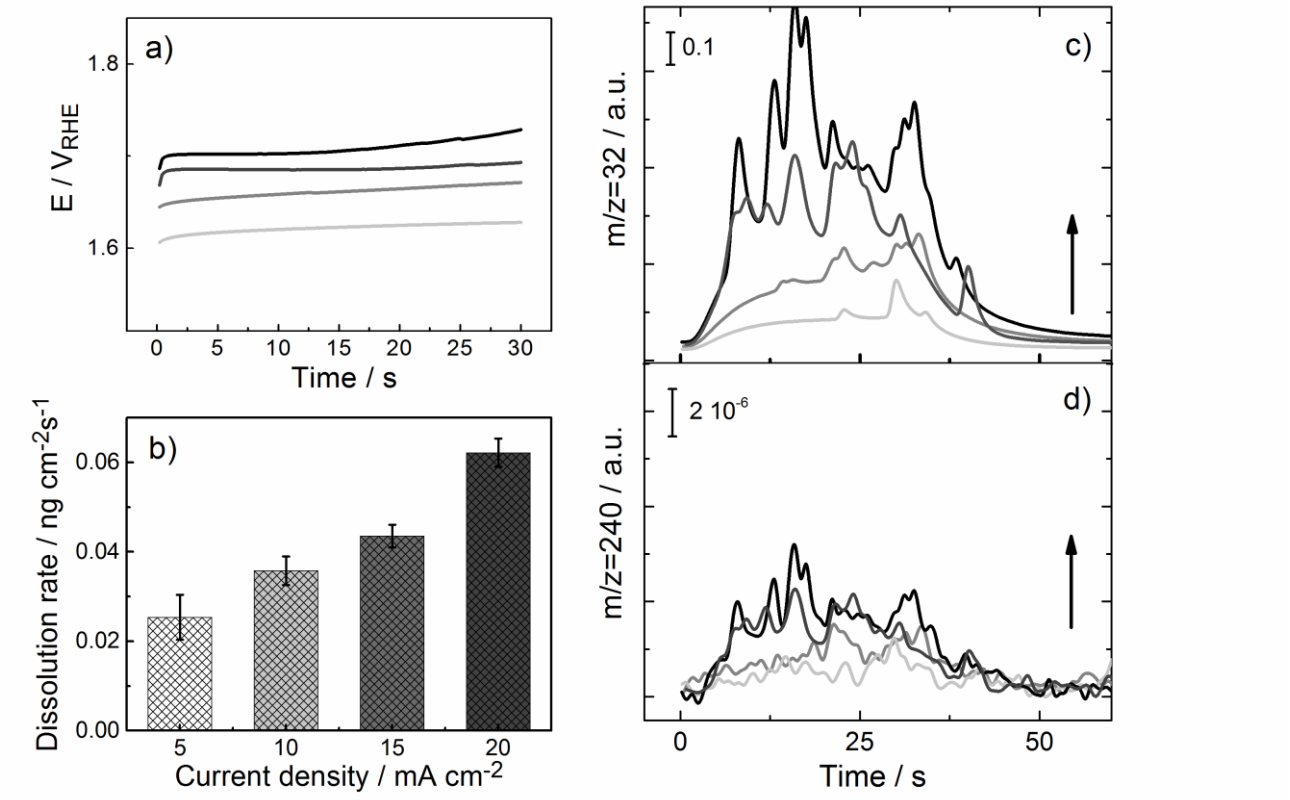

Figure S7. Direct observation of an intermediate of Ir dissolution during the OER. a) Measured potential during 30 s of anodic polarization of reactively sputtered IrO_2 in 0.1 M $HClO_4$ at 5, 10, 15 and 20 mA cm^{-2} at room temperature. b) Rate of iridium dissolution and signals of c) $^{32}O_2$ and d) $^{240}IrO_3$ measured online with a). Gradient of colour indicates increase of applied current density from 5 mA cm^{-2} till 20 mA cm^{-2}.

Possible reactions leading to Ir dissolution, according to Scheme 1 in the main text.

$Ir = Ir^{3+} + 3e$ (S1)

$Ir + 2H_2O = IrO_2 + 4\,H^+ + 4e$ (S2)

$Ir^{3+} + 2H_2O = IrO_2 + 4\,H^+ + e$ (S2a)

$IrO_2 + H_2O = IrO_2OH_{ads} + H^+$ (S3)

$IrO_2OH_{ads} = IrO_2OH + e$ (S4)

$2IrO_2OH = 2HIrO_2 + O_2$ (S5)

$HIrO_2 + 3H^+ = Ir^{3+} + 2H_2O$ (S6)

$HIrO_2 = IrO_2 + H^+ + e$ (S7)

$IrO_2OH = IrO_3 + H^+ + e$ (S8)

$2IrO_3 = 2IrO_2 + O_2$ (S9)

$IrO_3 + H_2O = IrO_4^{2-} + 2H^+$ (S10)

References

[1] aS. J. Freakley, J. Ruiz-Esquius, D. J. Morgan, *Surface and Interface Analysis* **2017**; bV. Pfeifer, T. E. Jones, J. J. Velasco Vélez, C. Massué, R. Arrigo, D. Teschner, F. Girgsdies, M. Scherzer, M. T. Greiner, J. Allan, M. Hashagen, G. Weinberg, S. Piccinin, M. Hävecker, A. Knop-Gericke, R. Schlögl, *Surface and Interface Analysis* **2016**, *48*, 261-273; cV. Pfeifer, T. E. Jones, J. J. Velasco Velez, C. Massue, M. T. Greiner, R. Arrigo, D. Teschner, F. Girgsdies, M. Scherzer, J. Allan, M. Hashagen, G. Weinberg, S. Piccinin, M. Havecker, A. Knop-Gericke, R. Schlogl, *Physical Chemistry Chemical Physics* **2016**, *18*, 2292-2296.

[2] aS. Cherevko, S. Geiger, O. Kasian, A. Mingers, K. J. J. Mayrhofer, *Journal of Electroanalytical Chemistry* **2016**, *773*, 69-78; bA. A. Topalov, I. Katsounaros, J. C. Meier, S. O. Klemm, K. J. Mayrhofer, *The Review of scientific instruments* **2011**, *82*, 114103.

[3] J.-P. Grote, A. R. Zeradjanin, S. Cherevko, K. J. J. Mayrhofer, *Review of Scientific Instruments* **2014**, *85*, 104101.

[4] aO. Kasian, S. Geiger, P. Stock, G. Polymeros, B. Breitbach, A. Savan, A. Ludwig, S. Cherevko, K. J. J. Mayrhofer, *Journal of The Electrochemical Society* **2016**, *163*, F3099-F3104; bR. Kötz, H. Neff, S. Stucki, *Journal of The Electrochemical Society* **1984**, *131*, 72-77.

[5] S. Cherevko, S. Geiger, O. Kasian, N. Kulyk, J.-P. Grote, A. Savan, B. R. Shrestha, S. Merzlikin, B. Breitbach, A. Ludwig, K. J. J. Mayrhofer, *Catalysis Today* **2016**, *262*, 170-180.